# Testing of a 6m Hybrid Glass/Carbon Fibre Powder Epoxy Composite Wind Blade Demonstrator

**Conference Paper** · September 2020

CITATIONS
0

READS
75

**10 authors**, including:

Christophe Floreani
The University of Edinburgh
**7** PUBLICATIONS **49** CITATIONS
SEE PROFILE

Fergus Cuthill
The University of Edinburgh
**3** PUBLICATIONS **0** CITATIONS
SEE PROFILE

James Maguire
The University of Edinburgh
**11** PUBLICATIONS **42** CITATIONS
SEE PROFILE

Conchur O'Bradaigh
The University of Edinburgh
**97** PUBLICATIONS **1,139** CITATIONS
SEE PROFILE

# Testing of a 6m Hybrid Glass/Carbon Fibre Powder Epoxy Composite Wind Blade Demonstrator

Christophe Floreani[1], Fergus Cuthill[1], Jeff Steynor[1], James Maguire[1], Edward D. McCarthy[1], Maarten J. Niessink[2], Sandro Di Noi[2], Lukas Wittevrongel[3], Tomas Flanagan[4], Conchúr M. Ó Brádaigh[1]

1- School of Engineering, Institute for Materials and Processes, The University of Edinburgh, Sanderson Building, King's Buildings, Edinburgh, EH9 3FB, Scotland, UK

2- Suzlon Energy Blade Technology, Jan Tinbergenstraat 290, 7559 ST Hengelo, Netherlands

3- MatchID, Deinsesteenweg 94A, 9031 Drongen, Belgium

4- EireComposites Teo, Údarás Industrial Estate An Choill Rua, Inverin, Co. Galway, Ireland

## ABSTRACT

This paper describes work carried out as part of the Horizon 2020 POWDERBLADE project aimed at developing large (60m+) commercial wind turbine blades. The aims of the project were to reduce blade cost and weight without compromising reliability and performance, by introducing a carbon/glass fibre hybrid composite spar and leveraging novel powder epoxy resin technology. A 6.0m torsion box demonstrator was designed by Suzlon Energy, manufactured by EireComposites, and tested by the University of Edinburgh. The tests followed the DNVGL-ST-0376 [12] blade test specification and applied four critical load cases identified during its design. The test cases were performed in ascending load order, after which the lowest load case was repeated. The torsion box demonstrated no reduction in stiffness or natural frequency throughout the test. This work gives a detailed description of the test program carried out to validate the torsion box design.

## 1. INTRODUCTION

Renewable energy sources have grown rapidly over the past decade to reduce the energy industry's reliance on fossil fuels. This has led to a rapid growth in onshore wind with 54.2 GW added in 2019 representing a 10% growth in total onshore capacity. Offshore wind energy added 4.7 GW in 2019, which corresponds to a 20% growth in total capacity [1]. As the wind energy sector has matured, the length of blades has grown in order to optimise project costs and performance with 99% of wind turbines installed in 2018 in the US having a diameter greater than 100m [2]. These larger turbines have led to an increase in capacity factor and have allowed the exploitation of lower wind speed sites [2].

The increase in blade dimensions has led to higher gravitational loads but also an increase in aerodynamic loads. Therefore, the use of carbon in wind turbine blades has been investigated as a way of reducing blade weight while increasing the stiffness. The improved fatigue properties of carbon fibre composites, compared to glass fibre composites, are of particular interest for wind turbine blades [3]. Ong et al. [4] showed that switching from a pure GFRP to CFRP blade would result in an 80% weight reduction but also a 150% increase in blade cost, while a hybrid carbon-glass blade containing 30% carbon would lead to a 50% weight reduction for a 90% increase in cost [4]. More recently, Griffin et al. showed that adding a carbon spar cap for a 100m GFRP blade led to a 16% increase in blade cost while the weight was reduced by 35% [5]. Large offshore wind turbines built by LM wind and GE with blade lengths of 88.4m and 107m respectively are using hybrid glass-carbon blades [6,7]. This shows that, despite the increase in cost, hybrid laminates can be beneficial in lowering the Levelised Cost of Energy (LCOE) of large wind turbines.

The POWDERBLADE project focuses on commercialisation of a composite materials technology that responds to the conflicting demands of the renewable energy sector for longer, lighter and more efficient blades at a lower cost. The POWDERBLADE consortium is led by EireComposites, a

manufacturer of advanced composites for the aerospace and renewables sectors with Suzlon Energy Blade Technology, a wind turbine manufacturer, The University of Edinburgh, as well as WestBIC (EU Business and Innovation Centre for Ireland's Border, Midlands and Western Region).

The aim of POWDERBLADE has been to bring to market large wind turbine blades (60m+) at a reduced weight and cost and with an increased reliability and performance. These improvements are accomplished by introducing a carbon/glass hybrid spar that will enable a weight reduction of 20% compared to a conventional glass fibre spar as well as by leveraging the powder epoxy technology to achieve an overall blade cost reduction of 20%. This can be realised since powder epoxy can be stored at room temperature, has low viscosity and exotherm [8,9,10] and enables one-shot curing of blades [11] resulting in a reduction of labour and tooling costs.

A 6.0m hybrid carbon/glass torsion box demonstrator using powder epoxy resin was designed by Suzlon and manufactured by EireComposites. The University of Edinburgh performed static structural testing of the demonstrator to certify this technology according to DNVGL-ST-0376 [12]. These tests were carried out to ensure that the demonstrator could handle the maximum load cases as defined in IEC 61400-22 [13] and GL2010 [14]. Four load cases were carried out, and the test measurements focused mainly on the glass to carbon transition region. This ensured that damage was detected in this crucial region.

# 2. BLADE DEMONSTRATOR DESIGN AND MANUFACTURING

The detailed blade design and manufacturing process of the blade demonstrator is outside the scope of this work and is not fully disclosed, as it is the intellectual property of Suzlon and EireComposites, respectively. However, an overview of the design and manufacturing process follows to give context to the blade testing.

## 2.1 Blade Design

The torsion box was designed as a 1/5th scale version of the first half (containing the root section) of a 60m blade resulting in a 6.0m long specimen structure. The profile of the aerofoil was scaled down from a real blade, with the trailing edge being cut off to form a straight rear web. The transition from the circular root to the D-shape profile takes place within the first 3 meters of the blade. The root section of the blade is made from glass fibre reinforced powder epoxy to avoid having to redesign the root connection mechanism and it transitions into a carbon fibre reinforced powder epoxy structure. This transition occurs between 2.5 and 3.5m from the blade root. The loads used during design were scaled down to obtain similar strain levels as in the full-scale blade. The IEC [13] and GL [14] standards define the load cases to consider for blade testing, and Suzlon identified the 4 most critical of these to be used as part of this demonstrator design.

A purpose-built design optimization algorithm incorporating a 3D FE shell model of the torsion box was developed by Suzlon to minimise the weight of the blade, while ensuring that first ply failure did not occur under any of the blade load cases and ensuring that the maximum tip displacement remained under 0.4m. The blade was divided into sections along its length but also around each aerofoil section. The ply layup was optimized for each individual section leading to a large weight saving compared to a non-optimized blade. Additional reinforcement layers were added around the point of load application 5.5 m from the root as well as around the root to account for stress concentrations.

## 2.2 Blade Manufacturing

The first half of the blade was manufactured using a unidirectional stitched glass fibre fabric with areal weight of 1150 gsm while the second half was manufactured using UD stitched carbon fibre fabric from Saertex with a weight of 882 gsm. Both fabrics were reinforced with powder epoxy and turned into prepreg layers by EireComposites. The fibre volume fraction was around 50% for the glass fibre and carbon fibre prepregs.

The first part of the manufacturing process was to machine plugs from high density tooling board using CNC machines. These were then coated with a sealant and a release agent before the two female mould halves were manufactured from glass fibre using the plugs. Figure 1 shows one of the mould halves following curing. A release agent was then applied to the mould surfaces prior to layup.

*Figure 1: Blade mould half after curing*

The two blade halves were then manufactured separately within each mould. After 30 layers had been placed, the two halves were placed under vacuum and B-staged to ensure the plies conformed to the shape of the mould. After the layup was completed, each torsion box half was B-staged again. Finally, both torsion box halves were placed back into the moulds and fully cured together in a process that ensured good bond strength and surface finish.

# 3. TEST SETUP

## 3.1 Test Objectives

The torsion box demonstrator testing consisted in subjecting the blade to the 4 load cases, which were used as a basis for the design structural optimisation. The main aims of this test were to:

- Ensure that the blade did not fail under the design loads
- Verify that no damage detrimental to the blade structure occurred during testing
- Measure the strains at 4 quadrants around the blade and at 5 different positions along the length.
- Measure the displacement at the loading point as well as the middle of the blade.
- Measure the natural frequency and blade damping.

## 3.2 Reaction Frame Design

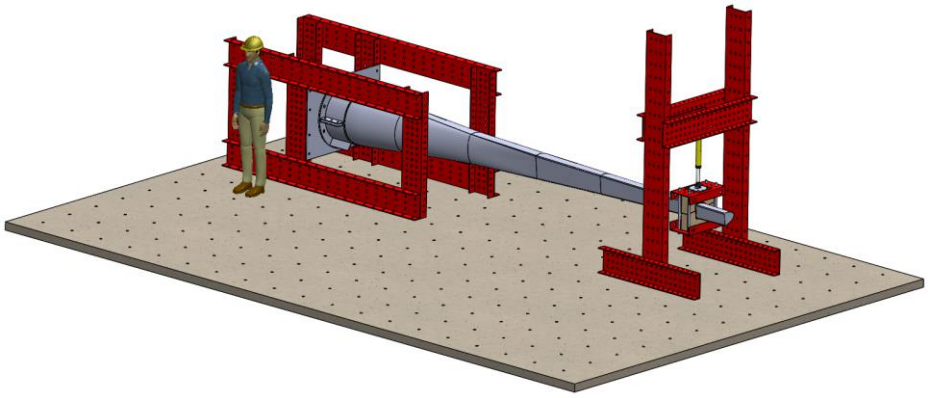

*Figure 2: Overview of reaction frame design*

C-channel steel beams were used for the construction of the main reaction frame. As shown in Figure 2, the beams were arranged to support the torsion box root connection and transfer the reaction forces and bending moments through a concrete strong floor (approx. 9 m x 6 m). Similarly, a frame was used to apply the test load to the torsion box loading connector, with the reaction forces also transferred to the strong floor.

### 3.3 Loading of the Demonstrator

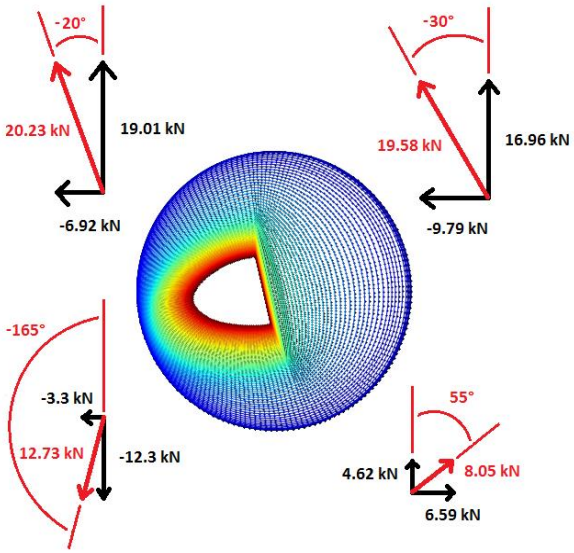


*Figure 3: Load case vectors with respect to the blade orientation. The blade is pointing out of the Plane*

The 4 load cases to be applied to the blade are summarized in Table 1 below. The orientation of the loads is shown in Figure 3 . The load cases were carried out in increasing load order (4,3,2,1). At the end of the test, the 4th load case will be repeated to verify the structural integrity has not changed (i.e. change in the load-strain response).

*Table 1: Combined loading vectors for each load case (LC).*

| Torsion Box | | | |
|---|---|---|---|
| LC | Angle [deg] | RBM [kNm] | Force at 5.5m [kN] |
| 1 | -20 | 111.29 | 20.23 |
| 2 | -30 | 107.7 | 19.58 |
| 3 | -165 | 70.04 | 12.73 |
| 4 | 55 | 44.26 | 8.05 |

All load cases were applied at a point 5.5 m from the root. For each load case, a unique loading connection was designed and machined from medium-density fibreboard (MDF), then fixed in place by rigid steel beams as shown in Figure 2. Neoprene rubber inlays (1.5 mm thick) were used to improve friction and reduce contact stresses between the composite and MDF. Loading was performed using a double-acting hydraulic actuator. The actuator was hinged to accommodate the out-of-plane deflection of the blade during testing. A 25 kN S-beam load cell was placed between the hydraulic actuator and the loading connection to record the applied load. The hydraulic actuator was attached to the reaction frame via a slot, which allowed it to slide sideways. This allowed loads to be applied up to an angle of 10° compared to the vertical direction.

### 3.4 Root Connection Design

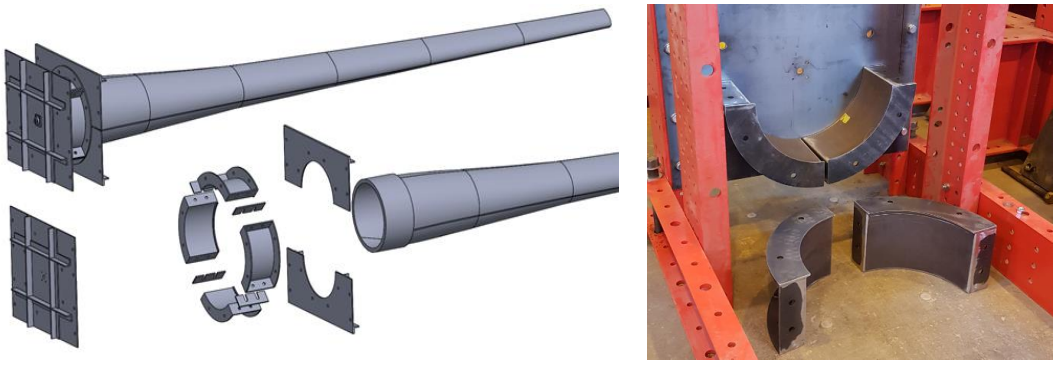

*Figure 4: Design for the torsion box root connection*

To withstand the bending moment, the root of the torsion box was clamped in position using a geometric locking arrangement (see Figure 4). The clamping fixture consisted of a backing plate, two front plates, and clamping plates that conformed to the blade root. In-depth finite element analysis (FEA) of the root connection was performed to ensure that slippage was kept to a minimum and that the final design did not suffer from any critical stress concentrations. The addition of a raised lip on the front flange of the clamp restricted the composite sleeve from slipping.

### 3.5 Data Logging

The main data outputs of the test were the applied load as well as the measured strain and blade displacement. The displacement was measured by both Qualisys motion tracking cameras and by two string potentiometers. Strain was measured by strain gauges as well as by Digital Imaging Correlation (DIC) in the transition region. Accelerometers were placed on the blade to measure natural frequency

and damping before and after each test run. Data was measured in both the loading and unloading steps.

### *3.5.1 Strain Gauges*

Strain gauges were positioned along four quadrants around the blade with one rosette strain gauge placed every metre from 1.0m to 5.0m from the root. This allowed strain to be measured at points of interest both along the length of the blade as well as around the blade profile using a total of 20 rosette strain gauges. The gauges were glued onto the blade and soldered to connecting wires. National Instruments data acquisition hardware was used to record the output of the gauges.

### *3.5.2 Digital Imaging Correlation*

Three sets of camera pairs were used to measure a 3D strain field at the glass-carbon transition (2.5 – 3.5 m) shown in Figure 5. The cameras were placed on, above, and on either side of the blade, and the strain map was measured using Digital Imaging Correlation software provided by MatchID. The presence of these three cameras enabled a full 3D strain mapping of the entire 360° around the transition area and hence allowed a precise strain measurement for the four load cases The transition region was first painted in white using a primer, and then a pattern of black dots, approximately 6mm in diameter, were sprayed unto the torsion box using a rubber mask. The DIC recorded the strain field around the torsion box and the DIC remained in the same location for each load case relative to the reaction frame i.e. it was not rotated with the torsion box.

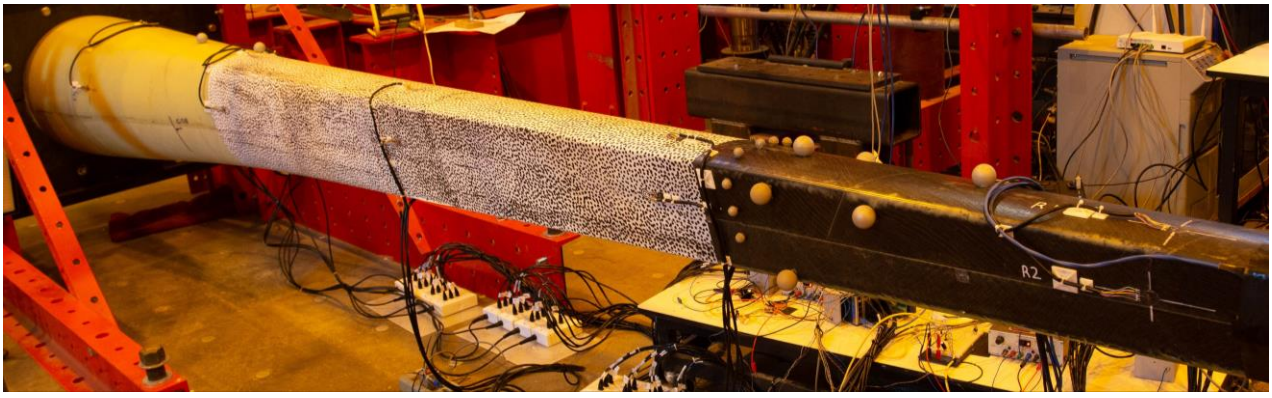


*Figure 5: Test setup showing transition area covered in white paint and speckling pattern for DIC*

### *3.5.3 Deflection Measurements*

Two string potentiometers were positioned along the torsion box to measure vertical deflection. One was placed on the hydraulic actuator to measure deflection at the point of load application, while the other one was placed near the mid-span of the torsion box (2830mm from the root).

Four Qualisys motion tracking cameras were positioned around the reaction frame to track the motion of markers (some are visible in Figure 5) placed on the blade. The system was calibrated to determine the initial relative distances between markers and their absolute positions in 3D space. To obtain an accurate measurement, it was essential to place markers in the field of view of as many cameras as possible, which is why four cameras were used. Markers were also placed around the hydraulic actuator to measure the angle of the ram during loading. This ensured that this angle did not deviate too much from the desired loading angle as the load was increased.

## 4. RESULTS AND ANALYSIS

### 4.1 Mass and COG Measurements

The S-beam load cell was removed from the hydraulic actuator and placed on a strap connected to the gantry crane located in the laboratory. A strap wrapped around the torsion box was then connected to the load cell and used to lift the blade. The strap was moved up and down the span until the blade was stable when lifted from a single point, identified as the centre of gravity (COG). The blade was

measured to have a weight of **117.8 ± 0.5 kg** and the COG was measured at **1570 ± 30 mm** from the root. The error on the COG location was relatively high because the friction between the strap and the blade meant it was difficult to find the exact COG location and the curvature of the blade then made it difficult to measure the exact distance from the COG line to the blade root.

### 4.2 Natural Frequency and Damping

Once attached and clamped to the test fixture, a free vibration analysis of the blade was carried out before and after each load case. A 3-axis accelerometer placed on the demonstrator was used to record data as the blade was pushed either vertically (X-Direction) or horizontally (Y-Direction). A fast Fourier transform (FFT) was carried out to obtain the frequency domain response of the acceleration data. The natural frequency of the blade could then be measured as the peak of the frequency domain response. A beating effect was noticed during free vibration of the blade and this was confirmed in the frequency domain by the presence of two peaks at 11.5 Hz in the X-direction and 12.2 Hz in Y-Direction. This is caused by the fact that the demonstrator is free to oscillate in both the horizontal and vertical directions which both have slightly different natural frequencies – the blade is stiffer in the flapwise direction. Free oscillation of the blade was carried out with the 73kg saddle attached and the damping ratio was calculated using the average damping ratio from cycles 30 to 100. The obtained damping ratio for the torsion box was 0.0031 ± 0.0006. Both the natural frequency and damping ratios of the torsion box remained constant throughout the test program.

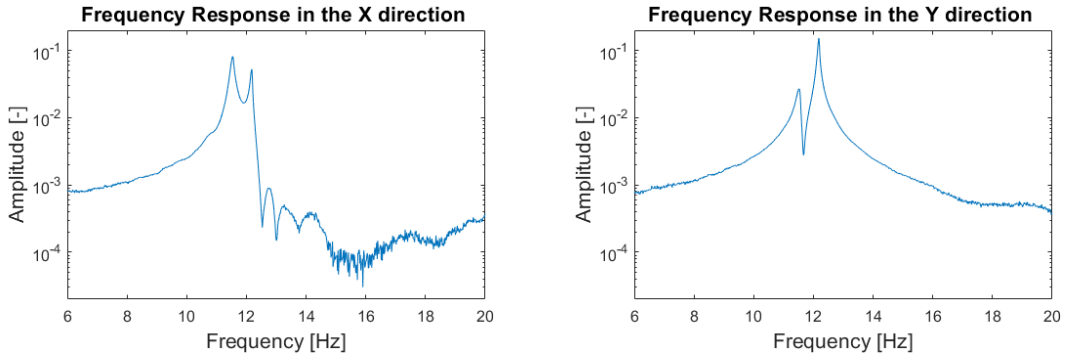


*Figure 6: Torsion box frequency response (left) in the x-direction (right) in the y-direction*

### 4.3 Strain Measurements

Using the rosette strain gauge data, the longitudinal, transverse and shear strains were obtained at each gauge location. The average strain value was then measured at the target test loads specified in Table 1. Figure 1 shows the longitudinal strain values obtained for all three test runs of Load Case 1. The black vertical lines in the plot represent the extremities of the transition region. The strain values show very good consistency between the three runs with the differences barely visible between the 3 tests. The strain values obtained in the repeat run of Load Case 4 were also all within 0.005% absolute strain of the ones obtained in the first run. Considering errors arising from slight differences in hydraulic actuator orientation as well as variations in the strain signal, this shows that negligible differences in the strain behaviour were observed between the two test runs.

The longitudinal strains were extracted using the MatchID 3D DIC software along the four quadrant lines where strain gauges were placed, allowing comparison between data from the strain gauges and from the DIC cameras by plotting the scattered DIC strain data against the interpolation of strain values between the strain gauges as shown on the right side of Figure 7. The DIC camera captured data from roughly 2050 mm to 3850mm from the root, and therefore measured an area slightly bigger than the transition region. However, it is important to note that at the edges of the areas used for strain mapping, difficulty in correlating the change in distances between speckles led to large overshoots of measured strain. The presence of the strain gauges, and especially the large cables used to connect them to the Data Acquisition hardware, also meant that large jumps in the measured strains were measured along

the quadrant lines by the DIC system. Aside from these discontinuities, DIC longitudinal strain was similar in magnitude at the strain gauge locations but showed nonlinear strain distribution between the gauges. This information allows the designer to perform a more precise comparison between the predicted and measured strains and the identification of ply drop locations.

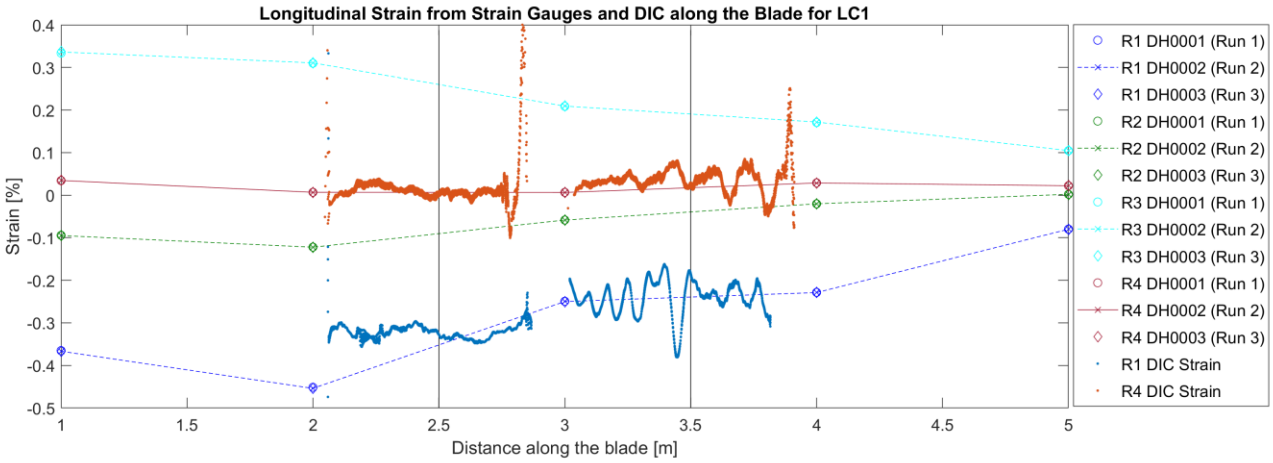


*Figure 7: Longitudinal strain from strain gauges along the torsion box including DIC strain results along the R1 and R4 strain gauge lines. Vertical Lines Outline the Transition Region*

### 4.4 Blade Deflection

The rotational stiffness of the test fixture was measured so that any apparent displacement of the blade tip caused by rotation of the frame near the root of the fixture could be removed. An A3 sheet was taped to the frame next to the hydraulic ram on which reference lines were drawn. A laser pointing towards the sheet was attached to the fixture near the blade root. Pictures were then captured throughout a first run of Load Case 4. The applied load in N as well as the laser were visible on these pictures. Using a CAD software, the distances could be measured between the reference line and the laser as a function of applied bending moment. Similarly, the width of the A3 sheet was measured and used to convert the vertical distance between the laser and the reference line into the real vertical distance. Doing so, and using trigonometry, the angle of rotation of the frame was measured as a function of the root bending moment. The frame rotation was linear to the applied moment, and it was found that the angular stiffness was equal to $5.94 * 10^{-5}\ rad/kNm$.

The corrected deflections were calculated at 5.5m from the root using both the data from the Qualisys markers as well as the string potentiometers. The displacement measurements, summarized in Table 2, were very consistent between the three runs of each load case and showed no perceptible difference between the initial Load Case 4 and the final repeat run. All the test runs showed a maximum displacement well under the maximum 0.4m allowed tip displacement, even when extrapolating the measured value of 5.5m to the tip displacement of the blade at 6.0m from the root.

*Table 2: Measured Displacement at 5.5m from the Root*

| Displacement at Load Application (5.5m from root) | Load Case 1 | Load Case 2 | Load Case 3 | Load Case 4 |
|---|---|---|---|---|
| | 119.4 mm | 162.8 mm | 235.0 mm | 240.9 mm |

### 4.5 Test Observations

Throughout the test program, no damage in the form of noise, cracks, delaminations, localised buckling of the torsion box or permanent deflections were observed for any of the load cases. No damage in any form was detected by either the strain gauges or the DIC cameras, which would have been identified by higher strain values for the repeat run of Load Case 4 in the event of damage. Additionally, maximum blade displacement as measured by Qualisys cameras and the string potentiometers show that the blade stiffness was the same at the start and end of the test program. Therefore, although it is

not possible to state that no damage occurred in the torsion box, it can be said that no damage detrimental to the blade structural properties was observed or measured throughout this test.

# 5. CONCLUSION

A test fixture was designed at The University of Edinburgh to test a 6.0m hybrid carbon/glass fibre powder epoxy composite blade. This demonstrator was designed by Suzlon and manufactured by EireComposites. 4 Load Cases identified by the blade designer as the most critical were applied and the blade was tested according to the DNVGL-ST-0376 [9] test specification. A purposely built root connection and an adjustable hydraulic actuator allowed loading of the blade in any direction. Strain was recorded throughout the blade using strain gauges and in the glass fibre to carbon fibre transition region using DIC software provided by MatchID. Displacement was measured using string potentiometers and motion tracking cameras, while the natural frequency and damping ratios were recorded using accelerometers during free vibration of the blade. The repeat run of Load Case 4 showed no increase in the measured strain or displacement compared to the first run. The natural frequency did not decrease during the test program. This shows that no reduction in the stiffness occurred throughout the test, which suggests that no damage detrimental to the integrity of the structure appeared while subjected to the 4 critical loads. The displacements measured during testing were also well under the maximum allowable 0.4m displacement. This test program therefore successfully validated the design of this novel blade and the recorded strains, displacements, natural frequencies, mass and damping values will serve as the basis for a comparison between the predicted and observed structural performance of the blade by Suzlon.

# 6. REFERENCES


1. IRENA, Renewable capacity statistics 2020 International Renewable Energy Agency (IRENA), Abu Dhabi, 2020
2. U.S. Department of Energy, "Wind Technologies Market Report", 2018.
3. Ong, C.-H.; Tsai, S.W. The Use of Carbon Fibers in Wind Turbine Blade Design: A SERI-8 Blade Example SAND2000-0478; Sandia National Laboratories Contractor Report; Sandia NL: Albuquerque, NM, USA, 2000.
4. Alam, P., Mamalis, D., Robert, C., Floreani, C., Ó Brádaigh, C.M.," The Fatigue of Carbon Fibre Reinforced Plastics - a Review", Composites Part B: Engineering, Vol. 166, pp. 555-579, 2019.
5. Griffith, D.T., "The SNL100-01 Blade: Carbon Design Studies for the Sandia 100-meter Blade,"Sandia National Laboratories Technical Report, SAND2013-1178, February 2013.
6. "Turbines of the year: Rotor blades", Windpowermonthly.com, 2020. [Online]. Available: https://www.windpowermonthly.com/article/1419306/turbines-year-rotor-blades. [Accessed: 07- May- 2020].
7. "GE Reveals World's Largest Wind-Turbine Blade", American Machinist, 2020. [Online]. Available: https://www.americanmachinist.com/news/article/21903042/ge-reveals-worlds-largest-windturbine-blade.
8. Maguire, J.M., Simacek, P., Advani, S.G. and Ó Brádaigh, C.M., "Novel epoxy powder for manufacturing thick-section composite parts under vacuum-bag-only conditions. Part I: Through-thickness process modelling", Composites Part A, September 2019
9. Maguire, J.M., Nayak, K. and Ó Brádaigh, C.M., "Novel epoxy powder for manufacturing thick-section composite parts under vacuum-bag-only conditions. Part II: Experimental validation", In Press, Composites Part A: Applied Science and Manufacturing, September 2019
10. J. M. Maguire, K. Nayak, and C. M. O Bradaigh, "Characterization of epoxy powders for processing thick-section composite structures," Materials & Design, vol. 139, pp. 112–121, 2018.
11. C. M. O Bradaigh, A. Doyle, D. Doyle, and P. J. Feerick, "Electrically-Heated Ceramic Composite Tooling for Out-of-Autoclave Manufacturing of Large Composite Structures",SAMPE Journal, vol. 47, no. 4, pp. 6–14, 2011.
12. DNV GL AS 2015 DNVGL-ST-0376 - Rotor blades for wind turbines
13. "IEC 61400-22 ed 1-0 b Wind Turbines Part 22 Conformity testing and certificiation," Edition 2010.
14. Germanischer Lloyd, "Guideline for the Certification of Wind Turbines Edition 2010_R1," Edition 2010.